

Hot news on the phase-structure of the SMEFT

Mikael Chala,* Maria Cristina Fiore,[†] and Luis Gil[‡]

Departamento de Física Teórica y del Cosmos, Universidad de Granada, E-18071 Granada, Spain

We perform dimensional reduction of the electroweak sector of the dimension-six SMEFT to order g^4 in coupling constants g . This analysis includes one-loop contributions to kinetic terms and quartic couplings; as well as two-loop contributions, where operators such as four-fermion interactions first appear, to squared mass terms. Using lattice data, we also provide evidence that, in contrast with previous statements in the literature, the SMEFT may undergo a first-order phase transition even for null $|\phi|^6$ at zero temperature, where ϕ is the Higgs doublet. This opens the door to entirely unexplored directions in model building.

I. INTRODUCTION

The modern approach to the study of high-temperature equilibrium phenomena within quantum field theory is based on the formalism of *dimensional reduction* (DR) [1, 2]. This method relies on the construction of a static, 3-dimensional (3D) effective-field theory (EFT), exploiting the hierarchy of scales between the temperature, T , and the masses, m , of light fields. In practice, all heavy Matsubara modes [3], with thermal masses of order πT , are integrated out in favor of a theory with light bosonic zero modes whose interactions encode all T dependence. Perturbative calculations in the 3D EFT framework can bypass numerous difficulties encountered within finite-temperature calculations in four dimensions (4D) [4]. Moreover, close to a critical point, where non-Abelian gauge theories become non-perturbative [5], the 3D dynamics can be simulated on the lattice [6–18].

For the Standard Model (SM), this 3D EFT is fully known to order g^4 [19], where $g \sim Y \sim \sqrt{\lambda}$ stand for the $SU(2)$, Yukawa and quartic couplings. (The full one-loop $\mathcal{O}(g^6)$ corrections have been computed in Ref. [20]; see also Ref. [21].) The phase structure of this theory was successfully understood on the lattice, with the remarkable finding that no first-order phase transition (FOPT) occurs within the electroweak sector of the SM [10, 22, 23]. This result, together with the future prospect of observing its imprint on a gravitational wave (GW) background [24–28], has motivated an extensive exploration of physics beyond the SM that can allow for a FOPT [17, 18, 20, 29–64].

As an alternative to a case-by-case analysis of viable SM extensions, some studies have taken a model-independent approach and explored the electroweak PT (EWPT) within the SMEFT [20, 41, 65]. The SMEFT is the most general EFT compatible with the gauge group of the SM, incorporating new decoupling physics effects in the form of non-renormalizable operators, parametrized in powers of an inverse energy cutoff Λ [66, 67]. This

framework enables a systematic investigation of the conditions under which a FOPT can emerge, and their connection with experimental input from colliders [68–73].

However, and despite the growing interest on the matter, little is yet known about the thermodynamics of the SMEFT. To the best of our knowledge, it is in Ref. [20] where the 3D EFT of the high-temperature SMEFT has been derived, at one loop and to order g^6 ¹. In this article, we extend Ref. [20] in two fronts. First, we include SMEFT operators, otherwise neglected in Ref. [20], that appear only at loop level in weakly-coupled ultraviolet (UV) completions of the SMEFT. And second, we compute the two-loop matching corrections of 3D mass terms. Altogether, we achieve for the first time full $\mathcal{O}(g^4)$ accuracy in the description of the SMEFT at high temperature. On the basis of this result and of up-to-date lattice data [17], we explore the possibility that the SMEFT undergoes a FOPT in regions of the parameter space previously overlooked in the literature.

The article is organized as follows. We introduce the SMEFT as well as our calculation techniques in section II. We dedicate sections IIA 1 and IIA 2 to discuss one-loop and two-loop matching conditions, respectively. Finally, relying on these results, we study the phase structure of the SMEFT in section III. We close with a discussion of our findings in section IV.

II. CALCULATION

We use the following conventions for the SMEFT Lagrangian:

$$\mathcal{L}_{\text{SMEFT}} = \mathcal{L}_{\text{SM}} + \frac{1}{\Lambda^2} \sum_i c_i \mathcal{O}_i + \mathcal{O}\left(\frac{1}{\Lambda^4}\right). \quad (1)$$

In this expression, Λ is a new physics scale, c_i are Wilson coefficients (WC) and the sum runs over the

¹ For SMEFT interactions, we assume that the power counting is $c_{X^3} \sim g$, $c_{X^2\phi^4} \sim c_{\phi^4 D^2} \sim c_{\psi^2 X\phi} \sim c_{\psi^2\phi^2} \sim c_{\psi^4} \sim g^2$, $c_{\psi^2\phi^3} \sim g^3$ and $c_{\phi^6} \sim g^4$; where we indicated the number of gauge field strength tensors (X), scalars (ϕ), fermions (ψ) and derivatives (D).

* mikael.chala@ugr.es

[†] mcristinafiore@ugr.es

[‡] lgil@ugr.es

X^3	
\mathcal{O}_{3G}	$f^{ABC} G_{\mu\nu}^A G_{\nu\rho}^B G_{\rho\mu}^C$
$\mathcal{O}_{3\bar{G}}$	$f^{ABC} \bar{G}_{\mu\nu}^A G_{\nu\rho}^B G_{\rho\mu}^C$
\mathcal{O}_{3W}	$\epsilon^{IJK} W_{\mu\nu}^I W_{\nu\rho}^J W_{\rho\mu}^K$
$\mathcal{O}_{3\bar{W}}$	$\epsilon^{IJK} \bar{W}_{\mu\nu}^I W_{\nu\rho}^J W_{\rho\mu}^K$
$X^2\phi^4$	
$\mathcal{O}_{\phi G}$	$(\phi^\dagger\phi) G_{\mu\nu}^A G^{A\mu\nu}$
$\mathcal{O}_{\phi\bar{G}}$	$(\phi^\dagger\phi) \bar{G}_{\mu\nu}^A G^{A\mu\nu}$
$\mathcal{O}_{\phi W}$	$(\phi^\dagger\phi) W_{\mu\nu}^I W^{I\mu\nu}$
$\mathcal{O}_{\phi\bar{W}}$	$(\phi^\dagger\phi) \bar{W}_{\mu\nu}^I W^{I\mu\nu}$
$\mathcal{O}_{\phi B}$	$(\phi^\dagger\phi) B_{\mu\nu} B^{\mu\nu}$
$\mathcal{O}_{\phi\bar{B}}$	$(\phi^\dagger\phi) \bar{B}_{\mu\nu} B^{\mu\nu}$
$\mathcal{O}_{\phi WB}$	$(\phi^\dagger\sigma^I\phi) W_{\mu\nu}^I B^{\mu\nu}$
$\mathcal{O}_{\phi\bar{W}B}$	$(\phi^\dagger\sigma^I\phi) \bar{W}_{\mu\nu}^I B^{\mu\nu}$
$\phi^4 D^2$	
$\mathcal{O}_{\phi\Box}$	$(\phi^\dagger\phi)\Box(\phi^\dagger\phi)$
$\mathcal{O}_{\phi D}$	$(\phi^\dagger D^\mu\phi)^\dagger\phi^\dagger D_\mu\phi$
ϕ^6	
\mathcal{O}_ϕ	$(\phi^\dagger\phi)^3$

TABLE I. Bosonic dimension-six SMEFT operators. Terms in gray arise at loop level in weakly-coupled UV completions.

$\psi^2 X\phi$	
\mathcal{O}_{uG}	$(\bar{q} T^A \sigma^{\mu\nu} u) \phi G_{\mu\nu}^A$
\mathcal{O}_{uW}	$(\bar{q} \sigma^{\mu\nu} u) \sigma^I \phi W_{\mu\nu}^I$
\mathcal{O}_{uB}	$(\bar{q} \sigma^{\mu\nu} u) \phi B_{\mu\nu}$
\mathcal{O}_{dG}	$(\bar{q} T^A \sigma^{\mu\nu} d) \phi G_{\mu\nu}^A$
\mathcal{O}_{dW}	$(\bar{q} \sigma^{\mu\nu} d) \sigma^I \phi W_{\mu\nu}^I$
\mathcal{O}_{dB}	$(\bar{q} \sigma^{\mu\nu} d) \phi B_{\mu\nu}$
\mathcal{O}_{eW}	$(\bar{l} \sigma^{\mu\nu} e) \sigma^I \phi W_{\mu\nu}^I$
\mathcal{O}_{eB}	$(\bar{l} \sigma^{\mu\nu} e) \phi B_{\mu\nu}$
$\psi^2 \phi^2$	
$\mathcal{O}_{\phi q}^{(1)}$	$\bar{q} \gamma^\mu q (\phi^\dagger i \overleftrightarrow{D}_\mu \phi)$
$\mathcal{O}_{\phi q}^{(3)}$	$\bar{q} \sigma^I \gamma^\mu q (\phi^\dagger i \overleftrightarrow{D}_\mu^I \phi)$
$\mathcal{O}_{\phi u}$	$\bar{u} \gamma^\mu u (\phi^\dagger i \overleftrightarrow{D}_\mu \phi)$
$\mathcal{O}_{\phi d}$	$\bar{d} \gamma^\mu d (\phi^\dagger i \overleftrightarrow{D}_\mu \phi)$
$\mathcal{O}_{\phi ud}$	$\bar{u} \gamma^\mu d (\phi^\dagger i \overleftrightarrow{D}_\mu \phi)$
$\mathcal{O}_{\phi l}^{(1)}$	$\bar{l} \gamma^\mu l (\phi^\dagger i \overleftrightarrow{D}_\mu \phi)$
$\mathcal{O}_{\phi l}^{(3)}$	$\bar{l} \sigma^I \gamma^\mu l (\phi^\dagger i \overleftrightarrow{D}_\mu^I \phi)$
$\mathcal{O}_{\phi e}$	$\bar{e} \gamma^\mu e (\phi^\dagger i \overleftrightarrow{D}_\mu \phi)$
$\psi^2 \phi^3$	
$\mathcal{O}_{u\phi}$	$\bar{q} \phi u (\phi^\dagger \phi)$
$\mathcal{O}_{d\phi}$	$\bar{q} \phi d (\phi^\dagger \phi)$
$\mathcal{O}_{e\phi}$	$\bar{q} \phi e (\phi^\dagger \phi)$

TABLE II. Two-fermion dimension-six SMEFT operators. Terms in gray arise at loop level in UV completions.

non-baryon-non-lepton-violating dimension-six operators of the SMEFT, that we reproduce for completeness in Tabs. I, II and III following the conventions of Refs. [67]. Pauli matrices are written as σ^I . We note that all operators denoted as \mathcal{O}_{fX} and $\mathcal{O}_{f\phi}$, where $f = u, d, e$ and $X = B, W, G$, are complex-valued.

q^4	
$\mathcal{O}_{qq}^{(1)}$	$(\bar{q} \gamma^\mu q) (\bar{q} \gamma_\mu q)$
$\mathcal{O}_{qq}^{(3)}$	$(\bar{q} \gamma^\mu \sigma^I q) (\bar{q} \gamma_\mu \sigma^I q)$
\mathcal{O}_{uu}	$(\bar{u} \gamma^\mu u) (\bar{u} \gamma_\mu u)$
\mathcal{O}_{dd}	$(\bar{d} \gamma^\mu d) (\bar{d} \gamma_\mu d)$
$\mathcal{O}_{ud}^{(1)}$	$(\bar{u} \gamma^\mu u) (\bar{d} \gamma_\mu d)$
$\mathcal{O}_{ud}^{(8)}$	$(\bar{u} \gamma^\mu T^A u) (\bar{d} \gamma_\mu T^A d)$
$\mathcal{O}_{qu}^{(1)}$	$(\bar{q} \gamma^\mu q) (\bar{u} \gamma_\mu u)$
$\mathcal{O}_{qu}^{(8)}$	$(\bar{q} \gamma^\mu T^A q) (\bar{u} \gamma_\mu T^A u)$
$\mathcal{O}_{qd}^{(1)}$	$(\bar{q} \gamma^\mu q) (\bar{d} \gamma_\mu d)$
$\mathcal{O}_{qd}^{(8)}$	$(\bar{q} \gamma^\mu T^A q) (\bar{d} \gamma_\mu T^A d)$
$\mathcal{O}_{quqd}^{(1)}$	$(\bar{q} u) \epsilon (\bar{q} d)$
$\mathcal{O}_{quqd}^{(8)}$	$(\bar{q} T^A u) \epsilon (\bar{q} T^A d)$
ℓ^4	
\mathcal{O}_{ll}	$(\bar{l} \gamma^\mu l) (\bar{l} \gamma_\mu l)$
\mathcal{O}_{ee}	$(\bar{e} \gamma^\mu e) (\bar{e} \gamma_\mu e)$
\mathcal{O}_{le}	$(\bar{l} \gamma^\mu l) (\bar{e} \gamma_\mu e)$
$q^2 \ell^2$	
$\mathcal{O}_{lq}^{(1)}$	$(\bar{l} \gamma^\mu l) (\bar{q} \gamma_\mu q)$
$\mathcal{O}_{lq}^{(3)}$	$(\bar{l} \gamma^\mu \sigma^I l) (\bar{q} \gamma_\mu \sigma^I q)$
\mathcal{O}_{eu}	$(\bar{e} \gamma^\mu e) (\bar{u} \gamma_\mu u)$
\mathcal{O}_{ed}	$(\bar{e} \gamma^\mu e) (\bar{d} \gamma_\mu d)$
\mathcal{O}_{qe}	$(\bar{q} \gamma^\mu q) (\bar{e} \gamma_\mu e)$
\mathcal{O}_{lu}	$(\bar{l} \gamma^\mu l) (\bar{u} \gamma_\mu u)$
\mathcal{O}_{ld}	$(\bar{l} \gamma^\mu l) (\bar{d} \gamma_\mu d)$
\mathcal{O}_{ledq}	$(\bar{l} e) (d q)$
$\mathcal{O}_{lequ}^{(1)}$	$(\bar{l} e) \epsilon (\bar{q} u)$
$\mathcal{O}_{lequ}^{(3)}$	$(\bar{l} \sigma^{\mu\nu} e) (\bar{q} \sigma_{\mu\nu} u)$

TABLE III. Four-fermion dimension-six SMEFT operators.

On the other hand, the SM Lagrangian reads:

$$\begin{aligned} \mathcal{L}_{\text{SM}} = & -\frac{1}{4} G_{\mu\nu}^A G^{A\mu\nu} - \frac{1}{4} W_{\mu\nu}^I W^{I\mu\nu} - \frac{1}{4} B_{\mu\nu} B^{\mu\nu} \quad (2) \\ & + \bar{q} i \not{D} q + \bar{l} i \not{D} l + \bar{u} i \not{D} u + \bar{d} i \not{D} d + \bar{e} i \not{D} e \\ & + (D_\mu \phi)^\dagger (D^\mu \phi) + \mu^2 |\phi|^2 - \lambda |\phi|^4 \\ & - (\bar{q} \phi Y_u u + \bar{q} \phi Y_d d + \bar{l} \phi Y_e e + \text{h.c.}), \end{aligned}$$

where u, d, e and q, l represent the right-handed quarks and leptons and their left-handed counterparts, respectively. Likewise, B, W and G stand for the gauge bosons, with g', g, g_S representing the corresponding gauge couplings. Finally, ϕ is the Higgs doublet, and $\phi = i\sigma_2 \phi^*$, and we use the minus sign convention for the covariant derivative.

Since we are studying the EWPT in the SMEFT, we shall assume that the temperature scale is much larger than all relevant mass scales, but lower than the new physics scale, i.e. $\Lambda \gg T \gg m$. In this situation, the SMEFT expansion remains valid while allowing for the standard [74] hierarchy of thermal scales:

$$\underbrace{\pi T}_{\text{hard}} \gg \underbrace{\left(\frac{g}{4\pi}\right) \pi T}_{\text{soft}} \gg \underbrace{\left(\frac{g}{4\pi}\right)^{3/2} \pi T}_{\text{supersoft}} \gg \underbrace{\left(\frac{g}{4\pi}\right)^2 \pi T}_{\text{ultrasoft}}, \quad (3)$$

written in terms of a weak coupling $g \ll 4\pi$.

A. From hard to soft scale

The first scale corresponds to the Matsubara modes of the SM fields, whose masses are of order πT , and which result from Fourier expanding around the compactified time dimension of radius $R \sim 1/T$ [3]. The second is associated to the screening of soft modes due to the hard-scale corrections, which induces a thermal mass for bosonic zero Matsubara modes. DR is the construction of the soft-scale 3D theory for zero Matsubara modes, and it amounts to integrating out all heavy non-zero modes. For the SM –in the presence of SMEFT interactions up to order g^4 – this 3D EFT, in Euclidean space, reads as follows [19]:

$$\mathcal{L}_3 = \mathcal{L}_3^{(m)} + \mathcal{L}_3^{(k)} + \mathcal{L}_3^{(\lambda)} + \mathcal{L}_3^{(\text{dim-6})} \quad (4)$$

with

$$\mathcal{L}_3^{(m)} = m_\phi^2 |\phi|^2 + \frac{1}{2} m_{B_0}^2 B_0^2 + \frac{1}{2} m_{W_0}^2 W_0^I W_0^I, \quad (5)$$

$$\begin{aligned} \mathcal{L}_3^{(k)} &= k_\phi (D_r \phi)^\dagger (D^r \phi) \\ &+ \frac{k_{B_0}}{2} (D_r B_0) (D^r B_0) + \frac{k_{W_0}}{2} (D_r W_0^I) (D^r W_0^I) \\ &+ \frac{k_B}{4} B_{rs} B_{rs} + \frac{k_W}{4} W_{rs}^I W_{rs}^I, \end{aligned} \quad (6)$$

and

$$\begin{aligned} \mathcal{L}_3^{(\lambda)} &= \lambda_{\phi^4} |\phi|^4 + \lambda_{B_0^4} B_0^4 + \lambda_{W_0^4} (W_0^I W_{0I})^2 \\ &+ \lambda_{\phi^2 B_0^2} |\phi|^2 B_0^2 + \lambda_{\phi^2 W_0^2} |\phi|^2 W_0^I W_{0I} \\ &+ \lambda_{B_0^2 W_0^2} B_0^2 W_0^I W_{0I} + \lambda_{\phi^2 B_0 W_0} B_0 \phi^\dagger \sigma^I \phi W_0^I. \end{aligned} \quad (7)$$

We denote by g_T and g'_T the 3D gauge couplings of $SU(2)$ and $U(1)$, respectively. We do not include gluons in the 3D EFT, as they do not couple directly to the Higgs, and their effect on the EWPT is thus expected to be subleading. Also, we abuse notation by denoting the 3D fields with the same symbols as their 4D counterparts.

The last piece, $\mathcal{L}_3^{(\text{dim-6})}$, includes all dimension-six operators² involving the Higgs and the gauge bosons in the 3D theory. According to our power counting, at order g^4 these arise only at tree level from their 4D counterparts. For brevity, we refrain from writing them here, as they will not be relevant for our results.

The parameters of the 3D EFT are computed upon requiring that Green's functions (namely off-shell correlators) in the 3D EFT reproduce the hard-region regime $Q^2 \sim (\pi T)^2 \gg P^2$, μ^2 of those obtained in the (compactified) 4D theory [75]. Here, Q and $P = (0, \mathbf{p})$ represent loop and static external momenta, respectively.

² Note that we count energy dimensions in 4D units always.

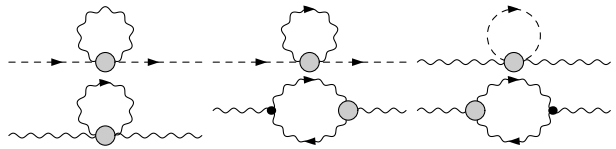


FIG. 1. Relevant diagrams for matching contributions to squared masses and kinetic terms by the operators in gray in Tables I and II at one loop. SMEFT vertices are represented as a gray circle.

To this aim, we use dedicated routines based on `FeynArts` [76] and `FeynCalc` [77]. We work in dimensional regularization with space-time dimension $d = 3 - 2\epsilon$ in the $\overline{\text{MS}}$ scheme, and use arbitrary R_ξ gauge. We only need the following sum-integral results:

$$I_{\alpha\beta\delta}^b \equiv \int_Q \frac{q_0^{2\beta} |\mathbf{q}|^{2\delta}}{Q^{2\alpha}}, \quad (8)$$

$$I_{\alpha\beta\delta}^f \equiv \int_{\{Q\}} \frac{q_0^{2\beta} |\mathbf{q}|^{2\delta}}{Q^{2\alpha}} = (2^{2\alpha-2\beta-2\delta-d} - 1) I_{\alpha\beta\delta}^b; \quad (9)$$

for $\beta \in \frac{1}{2}\mathbb{Z}$ and $\delta \in \mathbb{Z}$, with

$$\begin{aligned} I_{\alpha\beta\delta}^b &= \frac{(e^{\gamma_E} \bar{\mu}^2)^\epsilon}{8\pi^2} \times \frac{1 + (-1)^{2\beta}}{2} \times (2\pi T)^{1+d-2(\alpha-\beta-\delta)} \\ &\times \frac{\Gamma(\alpha - \frac{d}{2} - \delta) \Gamma(\frac{d}{2} + \delta) \zeta(2(\alpha - \beta - \delta) - d)}{\Gamma(\frac{1}{2}) \Gamma(\alpha) \Gamma(\frac{d}{2})}, \end{aligned} \quad (10)$$

where $\bar{\mu}$ is the renormalization scale.

All our results turn out to be ξ -independent and finite. The first statement is trivial; all 3D parameters are physical at order g^4 . It is only at higher-order that they receive corrections from 3D higher-dimensional operators which must be taken into account to achieve gauge independence in the physical basis [20, 60]. We have checked this is indeed true in all matching equations we present in the following.

The second statement can be understood as follows in the massless Higgs limit ($\mu^2 = 0$). Any divergences in the matching are either UV or infrared (IR). The UV ones can be accounted for by the running of the 4D renormalizable counterpart of 3D parameters; however dimensional analysis implies that these are not renormalized by SMEFT operators; see also Refs. [78–80]. On the other hand, IR divergences can be read from the UV divergences of the 3D EFT; but the running of 3D masses, which occurs first at two loops, involves no SMEFT coefficients at order g^4 ³. When including the Higgs mass,

³ Schematically, $m_\phi^2 \sim \lambda_{\phi^4}^2$, but

$$\lambda_{\phi^4} \sim \lambda T + (c_\phi + \lambda c_{\phi\Box} + \dots) T^2,$$

where the ellipses stand for other SMEFT contributions. Therefore, the running of m_ϕ^2 scales with powers like λc_ϕ or $\lambda^2 c_{\phi\Box}$, all of which are of order g^6 .

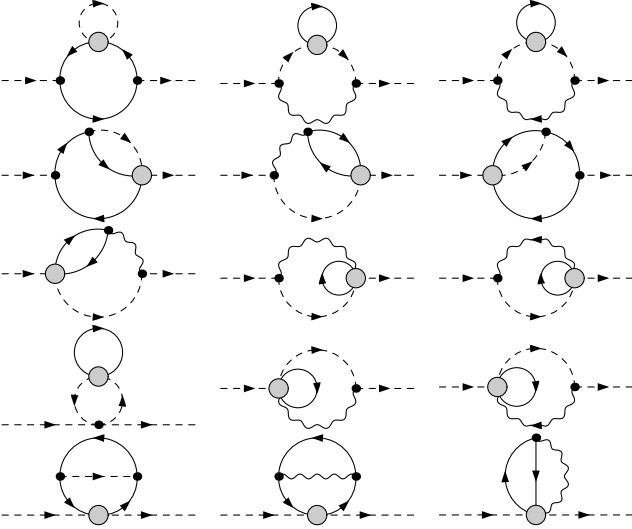


FIG. 2. Diagrams relevant for matching m_ϕ^2 by $\mathcal{O}_{\phi e}$ at two loops. SMEFT vertices are represented as a gray circle.

one can easily see that SMEFT operators do renormalize SM operators at one loop. However, our power counting shows that such divergences appear beyond order g^4 , so their effect on the running can be neglected.

1. One-loop results

At one loop, the non-vanishing SMEFT contributions to the 3D EFT read:

$$k_\phi = \frac{1}{12}(c_{\phi D} - 2c_{\phi\Box})T^2, \quad (11)$$

$$k_{B_0} = -\frac{2}{3}c_{\phi B}T^2, \quad (12)$$

$$k_{W_0} = -\frac{2}{3}(c_{\phi W} + 3gc_{3W})T^2, \quad (13)$$

$$k_B = -\frac{2}{3}c_{\phi B}T^2, \quad (14)$$

$$k_W = -\frac{2}{3}(c_{\phi W} + 3gc_{3W})T^2, \quad (15)$$

$$m_\phi^2 = \frac{1}{12}\mu^2(c_{\phi D} - 2c_{\phi\Box})T^2, \quad (16)$$

$$\lambda_{\phi^4} = \left[-c_\phi + \frac{1}{4}(g'^2 c_{\phi B} + g'gc_{\phi WB} + 3g^2 c_{\phi W}) + \lambda c_{\phi\Box} + \frac{1}{48}(3(g'^2 + g^2) - 16\lambda)c_{\phi D} - \frac{1}{12}(c_{e\phi} Y_e^* + 3(c_{d\phi} Y_d^* + c_{u\phi} Y_u^*) + \text{h.c.}) \right] T^3, \quad (17)$$

$$\lambda_{\phi^2 B_0^2} = \frac{1}{48}g'^2(6c_{\phi\Box} + 9c_{\phi D} - 8c_{\phi e} - 8c_{\phi l}^{(1)} + 16c_{\phi u} - 8c_{\phi d} + 8c_{\phi q}^{(1)})T^3, \quad (18)$$

$$\lambda_{\phi^2 W_0^2} = \frac{1}{48}g^2(6c_{\phi\Box} + c_{\phi D} + 8c_{\phi l}^{(3)} + 24c_{\phi q}^{(3)})T^3, \quad (19)$$

$$\lambda_{\phi^2 B_0 W_0} = \frac{1}{24}g'g(6c_{\phi\Box} + 5c_{\phi D} - 4c_{\phi e} - 4c_{\phi l}^{(1)} + 4c_{\phi l}^{(3)} + 8c_{\phi u} - 4c_{\phi d} + 4c_{\phi q}^{(1)} + 12c_{\phi q}^{(3)})T^3. \quad (20)$$

In order to avoid index clutter, we do not explicitly show the sum over generations in fermionic terms. The highlighted terms, which involve some of the operators that appear in gray in Tables I and II, were not included in Ref. [20] because these interactions arise at loop level in UV completions of the SMEFT. The corresponding diagrams relevant for matching the two-point functions are shown in Fig. 1 for an example.

2. Two-loop results

According to our power counting, only masses must be matched at two loops. We denote by Q and R the loop momenta. It can be shown that two-loop sum-integrals in our computation factorize trivially into one-loop masters. The reasoning is as follows. These sum-integrals, in their most general form, ensue from the 4D integrals

$$\frac{1}{\Lambda^2} \int \frac{d^4 Q d^4 R}{Q^{2\alpha} R^{2\beta} (Q-R)^{2\gamma}}.$$

Since we focus on squared mass terms, from dimensional analysis they must scale as $\sim T^4/\Lambda^2$, which in turn implies that $\alpha + \beta + \gamma = 2$. However, this is impossible if all exponents are positive, which is the only case where factorization is not immediate⁴.

We propose the following steps to factorize the two-loop sum-integrals:

(i) In terms with $Q + R$, we use the identity

$$Q \cdot R = \frac{1}{2} [(Q + R)^2 - Q^2 - R^2].$$

⁴ If one of the exponents is negative, then one can expand the numerator to transform the sum-integral into a sum of factorized ones. For example:

$$\not\int \frac{(Q-R)^2}{Q^4 R^4} = \frac{1}{2} \not\int \frac{Q^2 + R^2 - 2Q \cdot R}{Q^4 R^4} = \frac{1}{2Q^2 R^4} + \frac{1}{2Q^4 R^2};$$

where we have removed the term odd in Q and R (higher-powers of $Q \cdot R$ can be reduced to products of Q^2 and R^2 using tensor reduction). Had Q (or R) had the negative exponent, one could reach the same result upon changing variables $Q \rightarrow Q + R$. It is all this reasoning what we follow in this section.

- (ii) In terms with both $Q+R$ and Q (R) in the denominator, we perform the change of variables

$$Q+R \rightarrow R(Q).$$

We note that $Q+R$ is bosonic if both Q and R have the same statistics, but it is fermionic otherwise.

- (iii) At this stage, no term involves $Q+R$ anymore. Then we expand products of loop variables using

$$Q \cdot R = q_0 r_0 + \mathbf{q} \cdot \mathbf{r}.$$

- (iv) We set external Lorentz indices (μ, ν) to $(0, 0)$ or to (i, j) , depending on whether we match operators involving temporal or spatial components. We remove odd powers of q_0, r_0, \mathbf{q} and \mathbf{r} .
- (v) We use tensor reduction, $q_i r_j \rightarrow \frac{1}{d} \mathbf{q} \cdot \mathbf{r} \delta_{ij}$, where q_i (r_j) denotes the components of spatial loop momentum \mathbf{q} (\mathbf{r}).

Finally, we evaluate all one-loop integrals using the results in Eq. (10). Including all dimension-six SMEFT operators, we obtain:

$$\begin{aligned} m_\phi^2 = & \left[-\frac{1}{4}c_\phi + \frac{47}{3}g_S^2 c_{\phi G} + \frac{1}{576}|Y_u|^2(30c_{\phi\Box} - 15c_{\phi D} \right. \\ & + 6c_{\phi u} - 6c_{\phi q}^{(1)} + 18c_{\phi q}^{(3)} + 24c_{\phi u}^{(1)} + 32c_{\phi u}^{(8)}) \\ & \left. + \frac{3}{64}(16g_S c_{uG} Y_u^* - 3c_{u\phi} Y_u^* + \text{h.c.}) \right] T^4, \end{aligned} \quad (21)$$

where we have only included the limit where $\lambda, g, g', Y_d, Y_e \rightarrow 0$ for the sake of brevity ($m_{B_0}^2$ and $m_{W_0}^2$ get no correction in this limit). We provide the full result, including both one- and two-loop matching corrections, in the ancillary file `matching.txt`.

Example 1: Matching m_ϕ^2 by $\mathcal{O}_{\phi e}$

For the sake of clarity, we compute the contribution of $c_{\phi e}$ to m_ϕ^2 in the limit of vanishing g', g and λ and with only one family of fermions. To this aim, we consider the Green's function $\mathcal{G}_{\phi\phi}$ at zero momentum. The relevant Feynman diagrams are shown in Fig. 2. We obtain:

$$\begin{aligned} \mathcal{G}_{\phi\phi} & \sim 4 \sum_{\{QR\}} \left[\frac{1}{Q^2(Q+R)^2} + \frac{Q \cdot R}{Q^2 R^2 (Q+R)^2} \right] \\ & \stackrel{(i)}{=} 2 \sum_{\{QR\}} \left[\frac{1}{Q^2(Q+R)^2} + \frac{1}{Q^2 R^2} - \frac{1}{R^2(Q+R)^2} \right] \\ & \stackrel{(ii)}{=} 2 \left[\sum_{\{QR\}} \frac{1}{Q^2 R^2} + \sum_{\{QR\}} \frac{1}{Q^2 R^2} - \sum_{\{QR\}} \frac{1}{R^2 Q^2} \right]; \end{aligned} \quad (22)$$

where \sim indicates that we are ignoring the factor $c_{\phi e}|Y_e|^2$. Substituting the sum-integrals and taking into account that, in the 3D EFT, $\mathcal{G}_{\phi\phi} = m_\phi^2$, we therefore have:

$$\begin{aligned} m_\phi^2 & = -2c_{\phi e}|Y_e|^2 \left[I_{100}^b I_{100}^f + (I_{100}^f)^2 - I_{100}^f I_{100}^b \right] \\ & = -\frac{1}{288} c_{\phi e} |Y_e|^2 T^4, \end{aligned} \quad (23)$$

which is finite as expected.

Example 2: Matching $m_{B_0}^2$ by $\mathcal{O}_{\phi e}$

In this case, we take the limit of vanishing g and λ , still with only one family of fermions. The relevant diagrams are depicted in Fig. 3. We obtain:

$$\begin{aligned} \mathcal{G}_{BB} & \sim 8 \sum_{Q\{R\}} \left[-\frac{\delta_{\mu\nu}}{Q^2 R^2} + 2\frac{Q_\mu Q_\nu}{Q^4 R^2} + 2\frac{R_\mu R_\nu}{Q^2 R^4} \right. \\ & \quad \left. - 2\frac{(Q \cdot R)(Q_\mu R_\nu + R_\mu Q_\nu)}{Q^4 R^4} \right] \\ & \stackrel{(iii)}{=} 8 \sum_{Q\{R\}} \left[-\frac{1}{Q^2 R^2} + 2\frac{q_0^2}{Q^4 R^2} + 2\frac{r_0^2}{Q^2 R^4} \right. \\ & \quad \left. - 4\frac{q_0^2 r_0^2}{Q^4 R^4} \right] \end{aligned} \quad (24)$$

where now we are ignoring $g'^2 c_{\phi e}$. We therefore have:

$$\begin{aligned} m_{B_0}^2 & = -8g'^2 c_{\phi e} \left[-I_{100}^b I_{100}^f + 2I_{210}^b I_{100}^f \right. \\ & \quad \left. + 2I_{100}^b I_{210}^f - 4I_{210}^b I_{210}^f \right] \\ & = -\frac{1}{9} g'^2 c_{\phi e} T^4. \end{aligned} \quad (25)$$

B. From soft to supersoft scale

Temporal gauge bosons in the 3D EFT live at the soft scale, as they acquire positive squared masses proportional to $g^2 T^2$. However, close to the PT, the squared mass for the Higgs zero mode can be parametrically smaller, due to the approximate cancellation $m_\phi^2 \approx 0$ that occurs in the vicinity of the critical temperature. Thus, temporal gauge bosons can be integrated out to build a supersoft-scale EFT where only the Higgs zero-mode and the spatial, massless, gauge bosons are present.

In good approximation, given that $g' \ll g$, the contribution of the $U(1)$ gauge bosons to the Higgs effective potential is subleading compared to that of the $SU(2)$ ones. This motivates the construction of an $SU(2) +$ Higgs theory at the supersoft (SS) scale:

$$\begin{aligned} \mathcal{L}_{3,SS} & = \frac{1}{4} W_{rs}^I W_{rs}^I + (D_r \phi)^\dagger (D_r \phi) \\ & \quad + m_3^2 |\phi|^2 + \lambda_3 |\phi|^4 + \mathcal{L}_{3,SS}^{(\text{dim-6})}, \end{aligned} \quad (26)$$

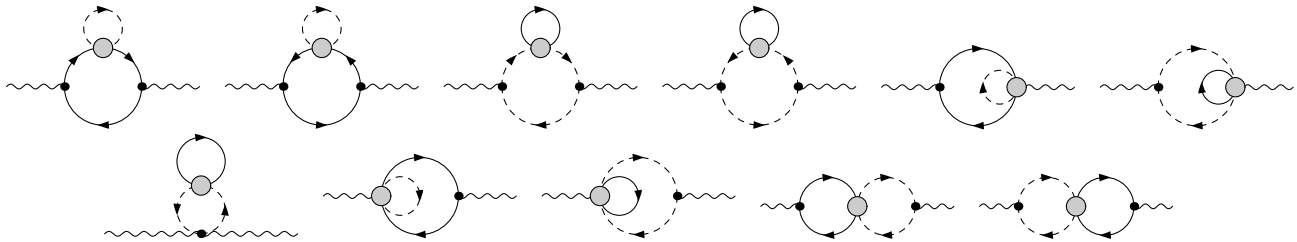


FIG. 3. Diagrams relevant for matching $m_{B_0}^2$ by $\theta_{\phi e}$ at two loops. SMEFT interactions are represented by a gray circle.

where we now dub g_3 the $SU(2)$ gauge coupling, and we again reuse the same names for the fields. $\mathcal{L}_{3,SS}^{(\dim-6)}$ encodes all dimension-six operators involving the W and ϕ fields in $d = 3$.

The construction of the supersoft EFT follows the standard procedure of matching between zero-temperature theories (T only appears in the WCs). The matching onto this theory was computed to order g^4 in Ref. [19], in the absence of higher-dimensional operators, starting from the SM in the high- T limit. In this work, we shall use these results and extend them with the contribution from SMEFT operators to the matching of the renormalizable parameters in the 3D EFT –Eqs. (11) to (20)–, and we will neglect the contribution from higher-dimensional operators where justified.

As it has long been understood, within perturbation theory one cannot go below the supersoft scale, as this theory suffers from the so-called Linde problem [5], which renders it non-perturbative at the *ultrasoft* scale. For this reason, an accurate prediction of the EWPT close to critical temperature demands the use of lattice methods, with input from perturbative physics at larger scales.

III. PHASE STRUCTURE

The phase structure of the theory described by the Lagrangian in Eq. (26) (in the absence of higher-dimensional operators) is studied on the lattice in terms of the dimensionless ratios $x \equiv \lambda_3/g_3^2$ and $y \equiv m_3^2/g_3^4$. As first determined in Ref. [22], the phase diagram presents a critical point located at $(x, y) = (x_*, y_*)$, with [10, 12]

$$x_* = 0.0983(15), \quad y_* = -0.0175(13), \quad (27)$$

for renormalization scale $\bar{\mu}_3 = g_3^2$ in the 3D EFT, which we also use.

We can roughly understand the evolution of the SM and the SMEFT across this phase diagram using $\mathcal{O}(g^2)$ matching in the limit of vanishing g' , together with generic deformations due to SMEFT interactions:

$$\begin{aligned} m_3^2 &= -\mu^2 + \frac{1}{4}(|Y_t|^2 + 3g^2 + 8\lambda)T^2 + \delta m_3^2 \frac{T^4}{\Lambda^2}, \\ \lambda_3 &= \lambda T + \delta \lambda_3 \frac{T^3}{\Lambda^2}, \\ g_3 &= g\sqrt{T}. \end{aligned} \quad (28)$$

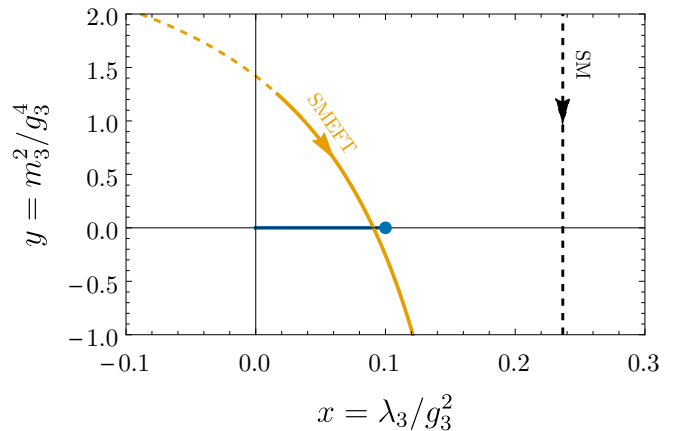


FIG. 4. Phase structure of the high-temperature limit of the SM and the SMEFT (for $\delta m_3^2 = -2$, $\delta \lambda_3 = -5.5$). The dot at the end of the blue line indicates a critical point. Transitions across this line are first-order.

Thus, for example, for $\delta m_3^2 = -2$, $\delta \lambda_3 = -5.5$, we obtain the phase diagram in Fig. 4, where we vaguely approximate the FOPT boundary with a straight segment $y = 0$. (As we show below, moderately sized WCs suffice when a more accurate description of the FOPT line and higher-order SM matching corrections are included.) We observe the well-known fact that the SM ($\delta m_3^2 = \delta \lambda_3 = 0$) shows a crossover, but for the SMEFT there can be a FOPT.

We assume $\Lambda = 1$ TeV, and the arrows in the figure indicate the temperature evolution from $T_i = \Lambda$ down to $T_f = 10$ GeV. The dashed region in the SMEFT line represents the temperatures at which the SMEFT is no longer a good approximation to the UV physics, $T \gtrsim \Lambda/(2\pi)$. Hereafter we assume that, at these temperatures, the UV physics is such that both x and y remain positive⁵.

The naive estimation above indicates that new physics mainly need to introduce a moderately negative correction to x (through a negative modification of λ_3 with respect to the SM value) in order to achieve a FOPT.

⁵ In fact, x can well be negative ($\lambda_3 < 0$) provided the potential is stabilized by other interactions (which might look like $\sim \phi^6$ in the EFT).

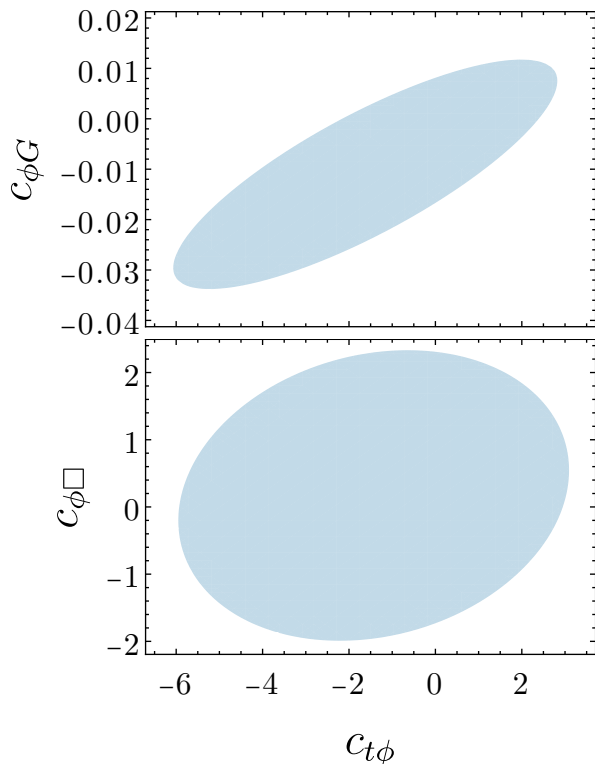


FIG. 5. Experimentally allowed values for $c_{t\phi}$ and $c_{\phi G}$, and for $c_{t\phi}$ and $c_{\phi\Box}$ in TeV^{-2} from top and Higgs physics [81–83], as derived using SMEFT upon marginalizing over other operators; see the text for details.

On the basis of Eqs. (11) to (20) and for concreteness, we focus on four particular operators in the SMEFT that can induce such shifts in λ_3 : $\mathcal{O}_{t\phi}$, $\mathcal{O}_{\phi G}$, \mathcal{O}_ϕ and $\mathcal{O}_{\phi\Box}$.

The first is somewhat constrained by Higgs data [81–83], though its bounds depend significantly on the second, $\mathcal{O}_{\phi G}$. Fig. 5 shows the ellipse of values of these WCs derived using SMEFT [84]⁶. We note that $\mathcal{O}_{t\phi}$ does not only affect λ_3 through its contribution to the matching, but also through a modification of the tree-level, zero temperature, relation between Y_t and the physical parameters. Indeed, one can easily find

$$m_t = \frac{Y_t v}{\sqrt{2}} + \frac{c_{t\phi} v^3}{2\sqrt{2}}, \quad (29)$$

where $m_t \sim 175$ GeV is the top mass and $v \sim 246$ GeV is the Higgs VEV. On the other hand, $\mathcal{O}_{\phi G}$ itself does not modify the PT, both because it only enters m_3^2 (at two-loop level), and because its value is tightly constrained.

The bounds on $\mathcal{O}_{t\phi}$ are such that it cannot allow for a FOPT alone, but an additional contribution to λ_3 from

different relatively unconstrained operators, such as \mathcal{O}_ϕ or $\mathcal{O}_{\phi\Box}$, is needed. The first of the two is not experimentally constrained, so we will take a conservative range of $[-1, 1] \text{ TeV}^{-2}$. On the other hand, in the plane of $c_{t\phi}$ and $c_{\phi\Box}$ upon marginalization, the latter is bounded as shown in Fig. 5.

These operators can also contribute significantly to the PT: \mathcal{O}_ϕ enters the matching of λ_ϕ at one loop, and $\mathcal{O}_{\phi\Box}$ enters the 3D EFT both through the quartic and the kinetic term of the 3D Higgs. They further modify the tree-level relation between μ^2 and λ and the physical parameters v and $m_H \sim 125$ GeV (see e.g. Ref. [85]) as:

$$\mu^2 = \frac{m_H^2}{2} + \frac{3}{4}c_\phi v^4 - 2c_{\phi\Box} \frac{m_H^2}{2} v^2, \quad (30)$$

$$\lambda = \frac{m_H^2}{2v^2} + \frac{3}{2}c_\phi v^2 - 4c_{\phi\Box} \frac{m_H^2}{2}, \quad (31)$$

at linear order in both WCs. We find these modifications to be particularly relevant, as generally $v > T_c$, where T_c is the critical temperature at which the FOPT takes place, so these contributions to the 3D parameters are less suppressed than the matching contributions.

In Figs. 6 and 7 we show the regions of the $c_{t\phi}$ - c_ϕ ($c_{\phi\Box} = 0$) and $c_{t\phi}$ - $c_{\phi\Box}$ ($c_\phi = 0$) planes of the parameter space, respectively, that allow for a FOPT and the corresponding value of $x = x_c$ for which it takes place. In contrast with the naive analysis in Fig. 4, here we rely on detailed lattice data. All points satisfy the following conditions:

1. The evolution curve of the SMEFT crosses the FOPT line, which is given by the fit formula in Eq. (13) in Ref. [17] for some $x < x_*$.
2. The evolution is from the symmetric phase towards the broken phase, that is, the curve goes to lower y as T decreases.
3. The crossing occurs at $\Lambda^2 > (\pi T)^2 > \mu^2$, so the hard-scale can be safely integrated out and the SMEFT description is valid.
4. At this T , we must have $m_\phi^2/m_{W_0}^2, m_\phi^2/m_{B_0}^2 < 0.5$, to guarantee the supersoft EFT expansion is under control.

We find remarkable that moderately positive values of $c_{t\phi}$, together with small negative values of c_ϕ or positive values of $c_{\phi\Box}$, drive the evolution towards the FOPT regime, both being allowed by experimental data⁷. In fact, if we combine the contribution from c_ϕ and $c_{\phi\Box}$,

⁶ We have marginalized over all the WCs that do *not* enter into Eqs. (11) to (20) in the limit of $g', g, \lambda, Y_e, Y_d \rightarrow 0$. (Powers of these SM parameters are so small that, together with the loop suppression, not even large values of the marginalized WCs affect significantly the matching conditions). All others are set to zero.

⁷ For all points considered, λ remains positive and (if present) c_ϕ is negative, so the zero-temperature potential is bounded from below at renormalizable and dimension-6 level. Also, we have $\lambda_3 > 0$, so the thermal potential barrier is radiative, and not tree-level generated [65].

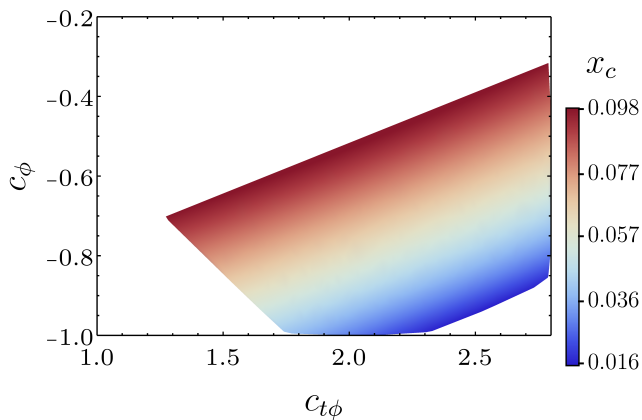


FIG. 6. Region of the $c_{t\phi}$ - c_{ϕ} parameter space (for fixed $c_{\phi\Box} = 0$) allowed by data that gives rise to a FOPT, and the corresponding value of x_c where the SMEFT evolution curve crosses the FOPT boundary, as extracted from Ref. [17]. The effect of varying $c_{\phi G}$ is negligible on the phase diagram, and it only influences the allowed values of $c_{t\phi}$, so we do not show it.

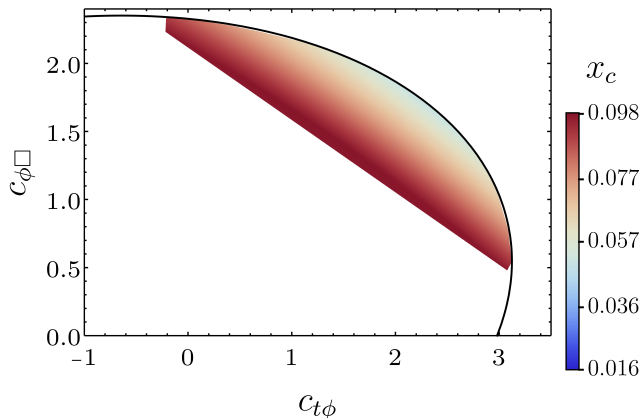


FIG. 7. Same as Fig. 6, but in the $c_{t\phi}$ - $c_{\phi\Box}$ plane (for fixed $c_{\phi} = 0$). We also show the ellipse with the experimentally allowed values for these WCs, from Fig. 5.

together with $c_{t\phi} \sim 2.5 \text{ TeV}^{-2}$, one can find a FOPT with both coefficients even below $\mathcal{O}(1) \text{ TeV}^{-2}$ in absolute value. The reason for all this is that, contrary to previous studies of the FOPT landscape of the SMEFT [41, 65, 69, 85–103], we have introduced $\mathcal{O}_{t\phi}$, which does not contribute directly to the Higgs potential at zero temperature, but enters the matching for λ_3 relatively unsuppressed. Together with the other two dimension-six terms, which contribute primarily through Eqs. (30) and (31), they all allow for smaller values of λ_3 and, thus, for smaller x ⁸.

We would also like to remark that the two-loop match-

ing corrections are essential for our results. Otherwise, the prediction for the parameter space where a FOPT can occur deviates significantly from the one derived here.

There is however a caveat in our analysis that we must address: the inclusion of \mathcal{O}_{ϕ} does modify the Higgs potential at tree-level, and thus also the potential in the supersoft theory in Eq. (26) through the $\mathcal{L}_{3,SS}^{(\text{dim-6})}$ piece. All lattice studies of the $SU(2) + \text{Higgs}$ theory have been carried out in the super-renormalizable case and, in particular, the FOPT boundary in Ref. [17] that we assume in this work does not consider modifications that break the super-renormalizability of the theory.

We claim, however, that this FOPT boundary should not be modified in the large x regime, as it corresponds to weaker transitions in the deep IR, i.e. closer to the critical temperature. One should however expect notable modifications due to higher-dimensional operators in the perturbative, small x regime, where FOPTs are stronger, as recently shown in Refs. [20, 52, 60, 62]. As discussed in Ref. [35], one can take $x > 0.01$ as an approximate regime where the inclusion of $(\phi^\dagger\phi)^3$ (as generated in the high- T limit of the SM) does not significantly alter the existing lattice results.

All in all, our results should give a good estimate of the weak FOPT landscape of the SMEFT, for x close to x_* . We shall leave a rigorous analysis of the effect of marginal operators in non-perturbative studies of the 3D $SU(2) + \text{Higgs}$ theory for future work.

Our findings open new avenues in model-building⁹, motivating the search for signatures of a FOPT in the early universe from beyond-the-SM models whose effect is not primarily to modify the Higgs potential directly (usually, extended scalar sectors).

IV. CONCLUSIONS

We have completed the dimensional reduction of the electroweak sector of the dimension-six SMEFT to full $\mathcal{O}(g^4)$ accuracy, demonstrating how the relevant two-loop sum-integrals can easily factorize into products of one-loop sum-integrals. Using existing lattice data, we have shown that the SMEFT can exhibit a first-order phase transition even without large modifications to the Higgs potential at zero temperature. Both one-loop and two-loop (for the square mass terms) matching corrections have been indispensable to arrive at this conclusion. This finding significantly expands the class of weakly-coupled, mass-gapped extensions of the Standard Model

⁸ The possibility of a near cancellation of λ_3 in the SMEFT was first noted in Appendix B in Ref. [65] as a curiosity. In the presence of c_{ϕ} only, which they study, it however requires too-large values of c_{ϕ} .

⁹ For instance, a possible UV completion that generates $c_{t\phi}$ consists of heavy vector-like quarks with quantum numbers $(\mathbf{3}, \mathbf{2})_{1/3}$ that couple only to the third family quarks through a mixed Yukawa term. (Scalar operators would come from loops enhanced by sizeable Yukawas among the Higgs and the new fermions, or by heavy scalars.). See e.g. Ref. [69].

⁸ The possibility of a near cancellation of λ_3 in the SMEFT was first noted in Appendix B in Ref. [65] as a curiosity. In the

that support a first-order phase transition, and motivates the search for collider signatures beyond the conventional targets of new light scalars or enhanced Higgs pair production [69, 71, 104–107].

ACKNOWLEDGMENTS

We acknowledge support from the MCIN/AEI (10.13039/501100011033) and ERDF (grants PID2021-128396NB-I00 and PID2022-139466NB-C22), from the Junta de Andalucía grants FQM 101 and P21-00199 and from Consejería de Universidad, Investigación e Innovación, Gobierno de España and Unión Europea – NextGenerationEU under grants AST22 6.5 and CNS2022-136024. MC and LG are further supported by the RyC program under contract number RYC2019-027155-I and by the FPU program under grant number FPU23/02026, respectively.

-
- [1] P. H. Ginsparg, Nucl. Phys. B **170**, 388 (1980).
 - [2] T. Appelquist and R. D. Pisarski, Phys. Rev. D **23**, 2305 (1981).
 - [3] T. Matsubara, Prog. Theor. Phys. **14**, 351 (1955).
 - [4] J. Löfgren, J. Phys. G **50**, 125008 (2023), arXiv:2301.05197 [hep-ph].
 - [5] A. D. Linde, Phys. Lett. B **96**, 289 (1980).
 - [6] K. Farakos, K. Kajantie, K. Rummukainen, and M. E. Shaposhnikov, Nucl. Phys. B **442**, 317 (1995), arXiv:hep-lat/9412091.
 - [7] K. Kajantie, M. Laine, K. Rummukainen, and M. E. Shaposhnikov, Nucl. Phys. B **466**, 189 (1996), arXiv:hep-lat/9510020.
 - [8] M. Laine, Nucl. Phys. B **451**, 484 (1995), arXiv:hep-lat/9504001.
 - [9] M. Laine and A. Rajantie, Nucl. Phys. B **513**, 471 (1998), arXiv:hep-lat/9705003.
 - [10] M. Gurtler, E.-M. Ilgenfritz, and A. Schiller, Phys. Rev. D **56**, 3888 (1997), arXiv:hep-lat/9704013.
 - [11] K. Rummukainen, M. Tsypin, K. Kajantie, M. Laine, and M. E. Shaposhnikov, Nucl. Phys. B **532**, 283 (1998), arXiv:hep-lat/9805013.
 - [12] M. Laine and K. Rummukainen, Nucl. Phys. B Proc. Suppl. **73**, 180 (1999), arXiv:hep-lat/9809045.
 - [13] G. D. Moore and K. Rummukainen, Phys. Rev. D **63**, 045002 (2001), arXiv:hep-ph/0009132.
 - [14] P. B. Arnold and G. D. Moore, Phys. Rev. E **64**, 066113 (2001), [Erratum: Phys.Rev.E 68, 049902 (2003)], arXiv:cond-mat/0103227.
 - [15] X.-p. Sun, Phys. Rev. E **67**, 066702 (2003), arXiv:hep-lat/0209144.
 - [16] M. D’Onofrio and K. Rummukainen, Phys. Rev. D **93**, 025003 (2016), arXiv:1508.07161 [hep-ph].
 - [17] O. Gould, S. Güyer, and K. Rummukainen, Phys. Rev. D **106**, 114507 (2022), [Erratum: Phys.Rev.D 110, 119903 (2024)], arXiv:2205.07238 [hep-lat].
 - [18] J. Annala, K. Rummukainen, and T. V. I. Tenkanen, (2025), arXiv:2506.04939 [hep-ph].
 - [19] K. Kajantie, M. Laine, K. Rummukainen, and M. E. Shaposhnikov, Nucl. Phys. B **458**, 90 (1996), arXiv:hep-ph/9508379.
 - [20] M. Chala and G. Guedes, JHEP **07**, 085, arXiv:2503.20016 [hep-ph].
 - [21] G. D. Moore, Phys. Rev. D **53**, 5906 (1996), arXiv:hep-ph/9508405.
 - [22] K. Kajantie, M. Laine, K. Rummukainen, and M. E. Shaposhnikov, Phys. Rev. Lett. **77**, 2887 (1996), arXiv:hep-ph/9605288.
 - [23] F. Csikor, Z. Fodor, and J. Heitger, Phys. Rev. Lett. **82**, 21 (1999), arXiv:hep-ph/9809291.
 - [24] G. M. Harry, P. Fritschel, D. A. Shaddock, W. Folkner, and E. S. Phinney, Class. Quant. Grav. **23**, 4887 (2006), [Erratum: Class.Quant.Grav. 23, 7361 (2006)].
 - [25] S. Kawamura *et al.*, Class. Quant. Grav. **23**, S125 (2006).
 - [26] W.-H. Ruan, Z.-K. Guo, R.-G. Cai, and Y.-Z. Zhang, Int. J. Mod. Phys. A **35**, 2050075 (2020), arXiv:1807.09495 [gr-qc].
 - [27] J. Aasi *et al.* (LIGO Scientific), Class. Quant. Grav. **32**, 074001 (2015), arXiv:1411.4547 [gr-qc].
 - [28] C. Caprini *et al.*, JCAP **03**, 024, arXiv:1910.13125 [astro-ph.CO].
 - [29] T. Brauner, T. V. I. Tenkanen, A. Tranberg, A. Vuorinen, and D. J. Weir, JHEP **03**, 007, arXiv:1609.06230 [hep-ph].
 - [30] J. O. Andersen, T. Gorda, A. Helset, L. Niemi, T. V. I. Tenkanen, A. Tranberg, A. Vuorinen, and D. J. Weir, Phys. Rev. Lett. **121**, 191802 (2018), arXiv:1711.09849 [hep-ph].
 - [31] L. Niemi, H. H. Patel, M. J. Ramsey-Musolf, T. V. I. Tenkanen, and D. J. Weir, Phys. Rev. D **100**, 035002 (2019), arXiv:1802.10500 [hep-ph].
 - [32] T. Gorda, A. Helset, L. Niemi, T. V. I. Tenkanen, and D. J. Weir, JHEP **02**, 081, arXiv:1802.05056 [hep-ph].
 - [33] K. Kainulainen, V. Keus, L. Niemi, K. Rummukainen, T. V. I. Tenkanen, and V. Vaskonen, JHEP **06**, 075, arXiv:1904.01329 [hep-ph].
 - [34] D. Croon, O. Gould, P. Schicho, T. V. I. Tenkanen, and G. White, JHEP **04**, 055, arXiv:2009.10080 [hep-ph].
 - [35] O. Gould, J. Kozaczuk, L. Niemi, M. J. Ramsey-Musolf, T. V. I. Tenkanen, and D. J. Weir, Phys. Rev. D **100**, 115024 (2019), arXiv:1903.11604 [hep-ph].
 - [36] L. Niemi, M. J. Ramsey-Musolf, T. V. I. Tenkanen, and D. J. Weir, Phys. Rev. Lett. **126**, 171802 (2021), arXiv:2005.11332 [hep-ph].
 - [37] O. Gould and J. Hirvonen, Phys. Rev. D **104**, 096015 (2021), arXiv:2108.04377 [hep-ph].
 - [38] O. Gould, JHEP **04**, 057, arXiv:2101.05528 [hep-ph].
 - [39] P. M. Schicho, T. V. I. Tenkanen, and J. Österman, JHEP **06**, 130, arXiv:2102.11145 [hep-ph].

- [40] L. Niemi, P. Schicho, and T. V. I. Tenkanen, Phys. Rev. D **103**, 115035 (2021), [Erratum: Phys.Rev.D 109, 039902 (2024)], arXiv:2103.07467 [hep-ph].
- [41] J. E. Camargo-Molina, R. Enberg, and J. Löfgren, JHEP **10**, 127, arXiv:2103.14022 [hep-ph].
- [42] L. Niemi, K. Rummukainen, R. Seppä, and D. J. Weir, JHEP **02**, 212, arXiv:2206.14487 [hep-lat].
- [43] A. Ekstedt, Phys. Rev. D **106**, 095026 (2022), arXiv:2205.05145 [hep-ph].
- [44] A. Ekstedt, O. Gould, and J. Löfgren, Phys. Rev. D **106**, 036012 (2022), [Erratum: Phys.Rev.D 110, 019901 (2024)], arXiv:2205.07241 [hep-ph].
- [45] S. Biondini, P. Schicho, and T. V. I. Tenkanen, JCAP **10**, 044, arXiv:2207.12207 [hep-ph].
- [46] P. Schicho, T. V. I. Tenkanen, and G. White, JHEP **11**, 047, arXiv:2203.04284 [hep-ph].
- [47] J. Löfgren, M. J. Ramsey-Musolf, P. Schicho, and T. V. I. Tenkanen, Phys. Rev. Lett. **130**, 251801 (2023), arXiv:2112.05472 [hep-ph].
- [48] O. Gould and C. Xie, JHEP **12**, 049, arXiv:2310.02308 [hep-ph].
- [49] M. Kierkla, B. Swiezewska, T. V. I. Tenkanen, and J. van de Vis, JHEP **02**, 234, arXiv:2312.12413 [hep-ph].
- [50] G. Aarts *et al.*, Prog. Part. Nucl. Phys. **133**, 104070 (2023), arXiv:2301.04382 [hep-lat].
- [51] L. Niemi, M. J. Ramsey-Musolf, and G. Xia, Phys. Rev. D **110**, 115016 (2024), arXiv:2405.01191 [hep-ph].
- [52] M. Chala, J. C. Criado, L. Gil, and J. L. Miras, JHEP **10**, 025, arXiv:2406.02667 [hep-ph].
- [53] R. Qin and L. Bian, JHEP **08**, 157, arXiv:2407.01981 [hep-ph].
- [54] O. Gould and P. Saffin, (2024), arXiv:2411.08951 [hep-ph].
- [55] J. Chakraborty and S. Mohanty, (2024), arXiv:2411.14146 [hep-th].
- [56] L. Niemi and T. V. I. Tenkanen, (2024), arXiv:2408.15912 [hep-ph].
- [57] M. Kierkla, P. Schicho, B. Swiezewska, T. V. I. Tenkanen, and J. van de Vis, (2025), arXiv:2503.13597 [hep-ph].
- [58] A. Bhatnagar, D. Croon, and P. Schicho, (2025), arXiv:2506.20716 [hep-ph].
- [59] J. López Miras and L. Gil, PoS **DISCRETE2024**, 089 (2025).
- [60] F. Bernardo, P. Klose, P. Schicho, and T. V. I. Tenkanen, (2025), arXiv:2503.18904 [hep-ph].
- [61] Y. Zhu, J. Liu, R. Qin, and L. Bian, Phys. Rev. D **112**, 015018 (2025), arXiv:2503.19566 [hep-ph].
- [62] M. Chala, L. Gil, and Z. Ren, (2025), arXiv:2505.14335 [hep-ph].
- [63] X.-X. Li, M. J. Ramsey-Musolf, T. V. I. Tenkanen, and Y. Wu, (2025), arXiv:2506.01585 [hep-ph].
- [64] P. Navarrete, R. Paatelainen, K. Seppänen, and T. V. I. Tenkanen, (2025), arXiv:2507.07014 [hep-ph].
- [65] E. Camargo-Molina, R. Enberg, and J. Löfgren, (2024), arXiv:2410.23210 [hep-ph].
- [66] W. Buchmuller and D. Wyler, Nucl. Phys. B **268**, 621 (1986).
- [67] B. Grzadkowski, M. Iskrzynski, M. Misiak, and J. Rosiek, JHEP **10**, 085, arXiv:1008.4884 [hep-ph].
- [68] F. P. Huang, P.-H. Gu, P.-F. Yin, Z.-H. Yu, and X. Zhang, Phys. Rev. D **93**, 103515 (2016), arXiv:1511.03969 [hep-ph].
- [69] T. Huang, J. M. No, L. Pernié, M. Ramsey-Musolf, A. Safonov, M. Spannowsky, and P. Winslow, Phys. Rev. D **96**, 035007 (2017), arXiv:1701.04442 [hep-ph].
- [70] I. Brivio and M. Trott, Phys. Rept. **793**, 1 (2019), arXiv:1706.08945 [hep-ph].
- [71] M. J. Ramsey-Musolf, JHEP **09**, 179, arXiv:1912.07189 [hep-ph].
- [72] G. Isidori, F. Wilsch, and D. Wyler, Rev. Mod. Phys. **96**, 015006 (2024), arXiv:2303.16922 [hep-ph].
- [73] J. Aebischer, A. J. Buras, and J. Kumar, (2025), arXiv:2507.05926 [hep-ph].
- [74] O. Gould and T. V. I. Tenkanen, JHEP **01**, 048, arXiv:2309.01672 [hep-ph].
- [75] E. Braaten and A. Nieto, Phys. Rev. D **51**, 6990 (1995), arXiv:hep-ph/9501375.
- [76] T. Hahn, Comput. Phys. Commun. **140**, 418 (2001), arXiv:hep-ph/0012260.
- [77] V. Shtabovenko, R. Mertig, and F. Orellana, Comput. Phys. Commun. **207**, 432 (2016), arXiv:1601.01167 [hep-ph].
- [78] E. E. Jenkins, A. V. Manohar, and M. Trott, JHEP **10**, 087, arXiv:1308.2627 [hep-ph].
- [79] E. E. Jenkins, A. V. Manohar, and M. Trott, JHEP **01**, 035, arXiv:1310.4838 [hep-ph].
- [80] R. Alonso, E. E. Jenkins, A. V. Manohar, and M. Trott, JHEP **04**, 159, arXiv:1312.2014 [hep-ph].
- [81] J. Ellis, M. Madigan, K. Mimasu, V. Sanz, and T. You, JHEP **04**, 279, arXiv:2012.02779 [hep-ph].
- [82] J. J. Ethier, G. Magni, F. Maltoni, L. Mantani, E. R. Nocera, J. Rojo, E. Slade, E. Vryonidou, and C. Zhang (SMET), JHEP **11**, 089, arXiv:2105.00006 [hep-ph].
- [83] J. de Blas, A. Goncalves, V. Miralles, L. Reina, L. Silvestrini, and M. Valli, (2025), arXiv:2507.06191 [hep-ph].
- [84] T. Giani, G. Magni, and J. Rojo, Eur. Phys. J. C **83**, 393 (2023), arXiv:2302.06660 [hep-ph].
- [85] M. Postma and G. White, JHEP **03**, 280, arXiv:2012.03953 [hep-ph].
- [86] X.-m. Zhang, Phys. Rev. D **47**, 3065 (1993), arXiv:hep-ph/9301277.
- [87] D. Bodeker, L. Fromme, S. J. Huber, and M. Seniuch, JHEP **02**, 026, arXiv:hep-ph/0412366.
- [88] C. Grojean, G. Servant, and J. D. Wells, Phys. Rev. D **71**, 036001 (2005), arXiv:hep-ph/0407019.
- [89] S. W. Ham and S. K. Oh, Phys. Rev. D **70**, 093007 (2004), arXiv:hep-ph/0408324.
- [90] C. Delaunay, C. Grojean, and J. D. Wells, JHEP **04**, 029, arXiv:0711.2511 [hep-ph].
- [91] B. Grinstein and M. Trott, Phys. Rev. D **78**, 075022 (2008), arXiv:0806.1971 [hep-ph].
- [92] P. H. Damgaard, A. Haarr, D. O'Connell, and A. Tranberg, JHEP **02**, 107, arXiv:1512.01963 [hep-ph].
- [93] J. de Vries, M. Postma, J. van de Vis, and G. White, JHEP **01**, 089, arXiv:1710.04061 [hep-ph].
- [94] R.-G. Cai, M. Sasaki, and S.-J. Wang, JCAP **08**, 004, arXiv:1707.03001 [astro-ph.CO].
- [95] M. Chala, C. Krause, and G. Nardini, JHEP **07**, 062, arXiv:1802.02168 [hep-ph].
- [96] J. Ellis, M. Lewicki, and J. M. No, JCAP **04**, 003, arXiv:1809.08242 [hep-ph].
- [97] J. Ellis, M. Lewicki, J. M. No, and V. Vaskonen, JCAP **06**, 024, arXiv:1903.09642 [hep-ph].
- [98] J. Ellis, M. Fairbairn, M. Lewicki, V. Vaskonen, and A. Wickens, JCAP **09**, 019, arXiv:1907.04315 [astro-

- ph.CO].
- [99] V. Q. Phong, P. H. Khiem, N. P. D. Loc, and H. N. Long, *Phys. Rev. D* **101**, 116010 (2020), arXiv:2003.09625 [hep-ph].
 - [100] K. Hashino and D. Ueda, *Phys. Rev. D* **107**, 095022 (2023), arXiv:2210.11241 [hep-ph].
 - [101] S. Kanemura, R. Nagai, and M. Tanaka, *JHEP* **06**, 027, arXiv:2202.12774 [hep-ph].
 - [102] R. Alonso, J. C. Criado, R. Houtz, and M. West, *JHEP* **05**, 049, arXiv:2312.00881 [hep-ph].
 - [103] V. K. Oikonomou and A. Giovanakis, *Phys. Rev. D* **109**, 055044 (2024), arXiv:2403.01591 [hep-ph].
 - [104] J. M. No and M. Ramsey-Musolf, *Phys. Rev. D* **89**, 095031 (2014), arXiv:1310.6035 [hep-ph].
 - [105] H.-L. Li, M. Ramsey-Musolf, and S. Willocq, *Phys. Rev. D* **100**, 075035 (2019), arXiv:1906.05289 [hep-ph].
 - [106] P. Basler, S. Dawson, C. Englert, and M. Mühlleitner, *Phys. Rev. D* **101**, 015019 (2020), arXiv:1909.09987 [hep-ph].
 - [107] L. Biermann, C. Borschensky, C. Englert, M. Mühlleitner, and W. Naskar, *Phys. Rev. D* **110**, 095012 (2024), arXiv:2408.08043 [hep-ph].